Plasma Sci. Technol. **24** (2022) 124019 (10pp) https://doi.org/10.1088/2058-6272/ac989b

Dynamic performance of linear electromagnetic actuators in a stray magnetic field: theoretical analysis and experimental verification

Rumeng WANG (王如梦), Yong YANG (杨勇), Shaoyu WANG (王绍宇) and Ming ZHANG (张明)*

International Joint Research Laboratory of Magnetic Confinement Fusion and Plasma Physics, State Key Laboratory of Advanced Electromagnetic Engineering and Technology, School of Electrical and Electronic Engineering, Huazhong University of Science and Technology, Wuhan 430074, People's Republic of China

E-mail: zhangming@hust.edu.cn

Received 13 August 2022, revised 20 September 2022
Accepted for publication 9 October 2022
Published 23 December 2022

Abstract

Linear electromagnetic actuators (LEAs) are widely used in tokamaks, but they are extremely sensitive to and are prone to fail in a high-strength stray magnetic field (SMF), which is usually a concomitant with tokamaks. In this paper, a multi-physics coupling analysis model of LEA, including magnetic field, electric circuit and mechanical motion, is proposed, and the dynamic characteristics of LEAs in SMFs are studied in detail based on the proposed model. The failure mechanism of LEAs in SMFs is revealed, and the influence of SMFs on the dynamic performance of LEAs is studied and quantified. It is shown that the failure threshold of the LEA selected in this work under the rated condition is 27 mT and 14 mT in the positive and negative direction, respectively. Under a typical SMF of 10 mT in the negative direction, the closing time of the LEA will be extended by 40%, while its opening time will be shortened by about 10%. Experimental tests are also conducted, which verify the validity of the proposed model and the analysis results. This paper provides a basis for the diamagnetic optimization design of LEA, and it is of great significance to ensure the reliable operation of the tokamak.

Keywords: linear electromagnetic actuator, stray magnetic field, dynamic performance, collision velocity

(Some figures may appear in colour only in the online journal)

1. Introduction

With the development of magnetic confinement fusion, the operating parameters of tokamak devices are getting higher and higher. The plasma current of next-generation tokamak devices will reach the level of 10 MA, and the confinement magnetic field will also grow to several Teslas [1]. Such high plasma currents and confinement magnetic fields will generate high stray magnetic fields (SMFs) around the tokamak device [2–4]. Taking the ITER tokamak, a typical representative of the next-generation tokamak, as an example, its plasma current will be 17 MA, and the confinement magnetic field will be 5.3 T [1]. The ITER organization conducted a SMF analysis that shows that 50 mT magnetic field contour will occupy a space with a radius over 25 m, where a lot of electrical and electronic devices will be mounted [2]. Such a high SMF will affect the reliable operation of electrical and electronic devices mounted around the tokamak, which will, in turn, affect the reliable operation of the tokamak device [5].

* Author to whom any correspondence should be addressed.

Magnetic field interference has become one of the major concerns of ITER, thus the ITER organization has conducted many immunity tests against magnetic field that cover common electrical and electronic devices such as electromagnetic relays, relays, power supply modules, converters, programmable logic controllers, circuit breakers, etc. The test procedures for the immunity tests have been written in accordance with the most pertinent IEC (International Electrotechnical Commission) standards (61000-4-8) manufacturing suggestions and practices [6]. Each device has undergone a variety of tests using a static magnetic field to evaluate how they will behave under various operating circumstances. In accordance with IEC 61000-4-8, a solenoid (0.5 m in diameter and 0.5 m in height) was used to generate a magnetic field with spatial homogeneity within ±3 dB in the volume housing the test devices [7]. The tests showed that electromagnetic relays and contactors are among the most sensitive devices to magnetic fields, which would fail when the SMF is over 16 mT [6, 7].

Electromagnetic relays and contactors belong to linear electromagnetic actuators (LEAs), which also include solenoid valves [8–10]. LEAs are widely used in tokamaks and theuir peripheral equipment, such as solenoid valves in gas injection systems, contactors in power distribution systems, and electromagnetic relays in control systems. However, they are extremely susceptible to SMF, which is a threat to the tokamak device. The ITER organization has paid close attention to this potential risk, and the effectiveness of using magnetic shields to reduce magnetic field interference was evaluated. However, the simulation results show that the effect of the magnetic shield is limited, even a 10 mm thick C-shaped shield can only weaken the magnetic field by 50%, and the electrical and electronic device will still fail [2]. Moreover, it is not practical to use the shielding cover on a large scale because of the economy and space occupation. Therefore, it is necessary to study the magnetic field interference of LEA and analyze the characteristics of LEA in SMF.

As a matter of fact, LEAs are widely used in industrial and civil applications. However, as strong SMF environments seldom exist in the aforementioned areas, more attention is paid to optimize the LEA structure to improve its performance [11–13], and a few scholars focus on the failure of LEAs in SMFs. Zhai *et al* investigated the effect of uniform static magnetic field on electromagnetic relay, but only the closing process was considered [14]. Yang *et al* conducted the research on the electromagnetic interference of twin-type relay, and the effect of the magnetic field generated by the relays on their properties was quantitatively investigated. However, the field strength is much less than the environmental magnetic field of tokamak devices [15]. In general, although there are studies on the effect of magnetic field on LEAs, most of them consider the case of its self-generated magnetic field. Moreover, most of the research focuses on the effect of SMF on the static properties of LEAs [16], but the dynamic characteristics are also important features of LEAs. For example, the action time of solenoid valve will affect the gas injection volume, and the action delay of relay will affect the performance of the protection system.

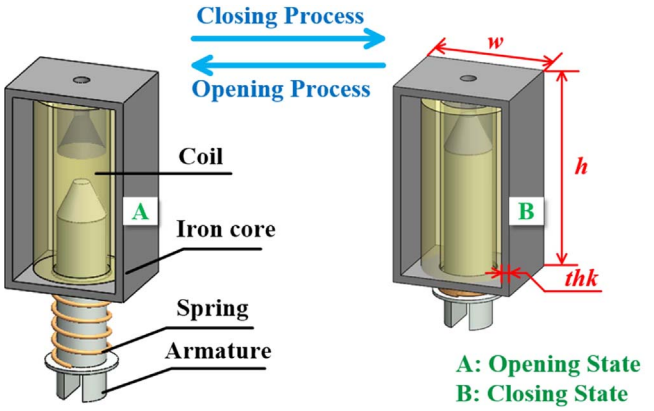

Figure 1. 3D model of the selected LEA (coil is shown as transparent).

This paper focuses on the dynamic performance of LEAs in SMFs, and proposes a multi-physics coupling model to analyze the influence of the SMF on the LEA. This paper is organized as follows. Section 2 presents the dynamic analysis model of a typical LEA in an SMF. The dynamic performance of LEA in an SMF is presented in section 3. Section 4 presents the experimental verification. Finally, a summary is provided in section 5.

2. Analysis model of LEAs in SMFs

As can be seen in figure 1, a typical LEA is selected in the analysis, which consists of iron core, armature, coil and spring. The iron core is 38 mm high, 30 mm wide, and 2.5 mm thick. The armature radius is 7.5 mm, height is 67 mm, and its max displacement is 22 mm. The core and armature are all ferromagnetic materials of the same material. The coil is 2150 turns, and the coil wire diameter is 0.4 mm. The elastic coefficient of the springs is 100 N m^{-1}, and the pre-compression distances is 10 mm. The rated voltage and current are 25 V and 0.84 A respectively, and the coil resistance is 29.8 Ω.

2.1. Mathematical model of LEAs

The operation of LEAs involves the coupling of electric circuit, magnetic field and mechanical motion. The whole operation can be divided into three processes, namely closing process, holding process and opening process. Figure 2 shows the simplified equivalent driving circuit of a LEA, in which the LEA is simplified as a variable inductance in the series with a resistor.

During the closing process, a driving current is fed to the LEA, and the governing equation of the electric circuit is

$$U(t) = R \cdot i(t) + \frac{\mathrm{d}[L \cdot i(t)]}{\mathrm{d}t} \tag{1}$$

where, $U(t)$ is the voltage cross the LEA coil, $i(t)$ is the coil current, R and L are the equivalent resistance and inductance of the LEA as shown in figure 1, respectively.

The closing process can be divided into two phases. In the first phase, the driving force increases as the coil current

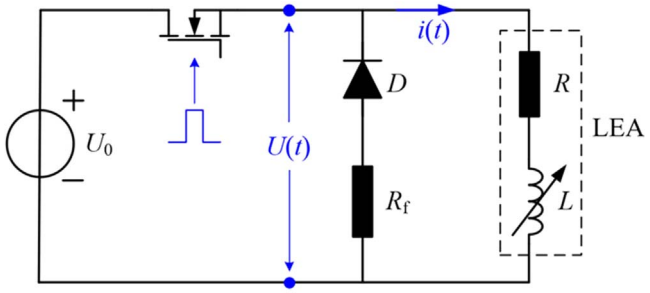

Figure 2. Simplified equivalent electric circuit of an LEA.

rises, but it is still smaller than the spring force as the spring is usually pre-compressed. During this phase, the armature remains still at the initial position. In the second phase, the driving force is larger than the spring force, and the armature will start to move. If ignoring the frictional force, its motion equation during the closing process can be expressed as

$$\begin{cases} s(t) = 0, & F_{\mathrm{EM}} \leqslant F_{\mathrm{f}} \\ m\dfrac{\mathrm{d}^2 s(t)}{\mathrm{d}t^2} = F_{\mathrm{EM}} - F_{\mathrm{f}}, & F_{\mathrm{EM}} > F_{\mathrm{f}} \end{cases} \tag{2}$$

where, $s(t)$ is the displacement of the armature, m is the armature mass, F_{EM} is the electromagnetic force applied on the armature, and F_{f} is the spring force, which can be expressed as

$$F_{\mathrm{f}} = k[s(t) + d] \tag{3}$$

where, k is the elastic coefficient of the spring, and d is the pre-compressed distance of the spring. It can be observed in equation (2) that the armature starts to move when the driving force and the spring force come to a balance, and the coil current at this time is called the starting current in this paper.

At the end of the closing process, if the electromagnetic holding force is greater than the spring force, the armature will remain in the final position, which is called the contact point. During the holding process, the governing equation of the electric circuit can be also expressed in equation (1). However, the supplied voltage to the coil is usually chopped to ensure that the holding force is slightly larger than the spring force for low energy consumption purposes. The armature remains still at the contact point, and its motion equation can be expressed as

$$s(t) = s_{\max}. \tag{4}$$

The opening process starts when the supplied voltage is removed. The coil current will flow through the freewheel diode, and the electric circuit equation will be

$$(R + R_{\mathrm{f}}) \cdot i(t) + \frac{\mathrm{d}[L \cdot i(t)]}{\mathrm{d}t} = 0 \tag{5}$$

where R_{f} is the resistance in the freewheel branch, which is usually employed to speed up the current decay and the armature release.

The armature motion during this period can be also divided into two phases. In the first phase, the holding force is still larger than the spring force and the armature will remain at the contact point. In the second phase when the holding force is small than the spring force, the armature will be pulled back to the initial position. Thus, the motion equation during the opening process can be expressed as

$$\begin{cases} s(t) = s_{\max}, & F_{\mathrm{EM}} \geqslant F_{\mathrm{f}} \\ m\dfrac{\mathrm{d}^2 s(t)}{\mathrm{d}t^2} = F_{\mathrm{EM}} - F_{\mathrm{f}}, & F_{\mathrm{EM}} < F_{\mathrm{f}}. \end{cases} \tag{6}$$

The release of armature starts when the holding force and the spring force come to a balance, and the coil current at this time is called the release current in this paper.

The Maxwell equation is used to describe the magnetic field of the LEA,

$$\nabla \cdot \boldsymbol{B} = 0 \tag{7}$$

$$\nabla \times \boldsymbol{H} = \boldsymbol{J} \tag{8}$$

where $\boldsymbol{B}$ is the magnetic induction, $\boldsymbol{H}$ is the magnetic field and $\boldsymbol{J}$ is the current density. To solve the equation, the vector magnetic potential $\boldsymbol{A}$ is introduced as

$$\boldsymbol{B} = \nabla \times \boldsymbol{A}. \tag{9}$$

The driving force and equivalent inductance are two key parameters that govern the dynamic characteristics of the LEA as shown in equations (1) and (2), and they can be obtained by solving equations (7)–(9). The inductance is calculated by energy method as

$$W = \frac{1}{2}Li^2 = \frac{1}{2}\int_{\Omega} \boldsymbol{B} \cdot \boldsymbol{H}\mathrm{d}\Omega \tag{10}$$

where W is the energy stored in the inductor. Assuming a unit current, the equivalent inductance can be expressed as

$$L = \int_{\Omega} \boldsymbol{B} \cdot \boldsymbol{H}\mathrm{d}\Omega. \tag{11}$$

The electromagnetic force is calculated by virtual displacement method as

$$F_{\mathrm{em}} = \frac{\mathrm{d}W(i,\, s)}{\mathrm{d}s}\bigg|_{i=\mathrm{const}} = \frac{\partial}{\partial s}\left[\int_{\Omega}\left(\int_0^H \boldsymbol{B} \cdot \mathrm{d}\boldsymbol{H}\right)\mathrm{d}\Omega\right] \tag{12}$$

The finite element method is used to solve the equations. Due to the symmetry, a $1/4$ model is built for the analysis as shown in figure 3. The model consists of an LEA and a pair of magnetic field generation coils to simulate the background field. The magnetic field generation coils consist of two identical and coaxial oils with an inner diameter of 189 mm and an upper and lower distance of 157 mm according to the formula given in [17], and the cross-section is assumed to be 20 mm × 20 mm. The coils can generate a magnetic field with the inhomogeneity of 1.05, and the field generation efficiency is 4.8 mT/kA. The external magnetic field is adjusted by simply changing the current in the magnetic field generation coils. As a $1/4$ model is used, the magnetic field is assumed to be parallel on the symmetry boundary, which can be expressed as

$$\boldsymbol{n} \cdot \boldsymbol{H} = 0 \tag{13}$$

where, $\boldsymbol{n}$ is the normal unit vector of the symmetry boundary.

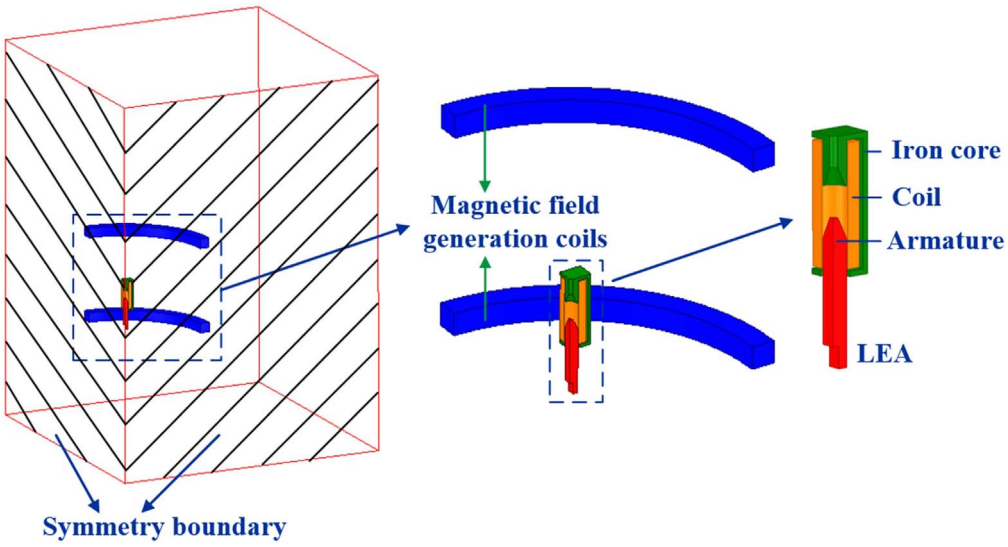

Figure 3. Finite element model of the LEA.

2.2. Influence on driving force and equivalent inductance

Analysis shows that the additional electromagnetic force exerted by the SMF on the LEA varies with the SMF direction, and it increases as the angle between the SMF and the central axis of the LEA decreases [9]. This means that the SMF parallel to the LEA axis has the greatest effect on the LEA, thus only this case is analyzed in this paper.

In equations (1)–(6), driving force (F_{EM}) and equivalent inductance (L) are key parameters that determine the dynamic characteristics of LEAs, and they are usually expressed as functions of driving current (i) and displacement (s) [18, 19]. Usually, analytical expressions can be obtained for equivalent inductance and driving force under certain assumptions based on the equivalent magnetic circuit method [20–26]. For complex problems, the finite element method can be used to obtain the distribution of driving force and equivalent circuit with respect to driving current and displacement. If the LEA is exposed to SMF (B_s), the driving force and equivalent inductance will be deviated, and it will certainly impact the dynamic performance of the LEA. Thus, the influence of the SMF on the driving force and equivalent circuit is discussed first. As the flux saturation and leakage is very complex when the SMF is included, and analytical expressions are not easy to find, the finite element method is employed in the analysis.

Figure 4 shows the distribution of driving force and equivalent inductance with respect to coil current and displacement. The maximum displacement considered in the analysis is 22 mm, and the maximum coil current is 1 A. The driving force increases with the driving current and displacement, while the equivalent inductance increases with displacement but decreases with driving current.

Figure 5 shows the electromagnetic force exerted on the armature by the SMF with different displacements while the LEA is not energized. It is shown that the force generated by SMF increases with the field strength. In most parts of the displacement, the force is in the reversed direction, which will slow down or even retard the motion of the armature.

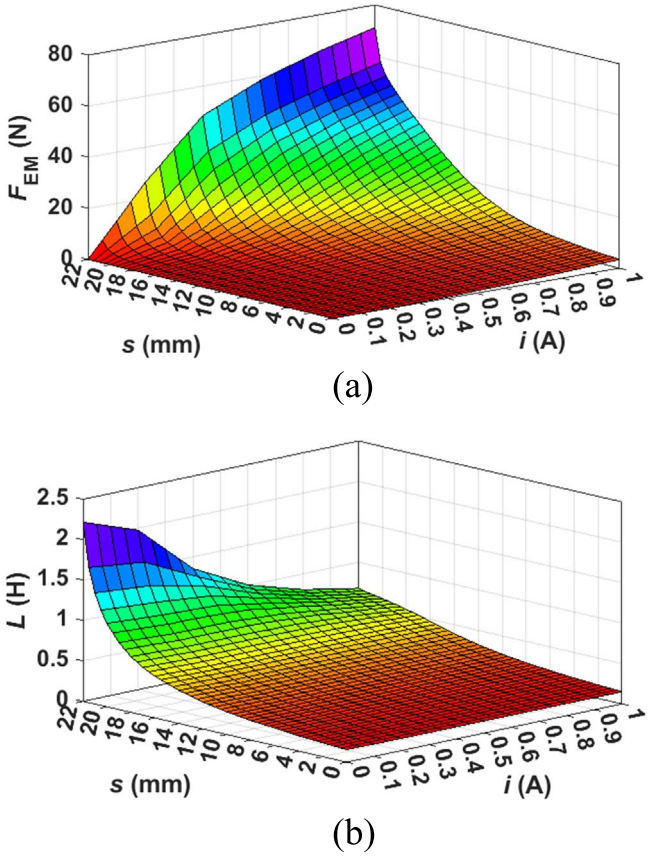

Figure 4. Distribution of driving force (F_{EM}) and equivalent inductance (L) with respect to displacement (s) and coil current (i) with no SMF (a) $F_{\mathrm{EM}}(i, s)$, (b) $L(i, s)$.

However, at the holding stage when $s = 22$ mm, the force exerted on the armature will turn to positive, and it will influence the reposition of the armature when the driving current is removed. Moreover, if the force generated by the SMF is larger than the spring force, the armature cannot be pulled back during the opening process.

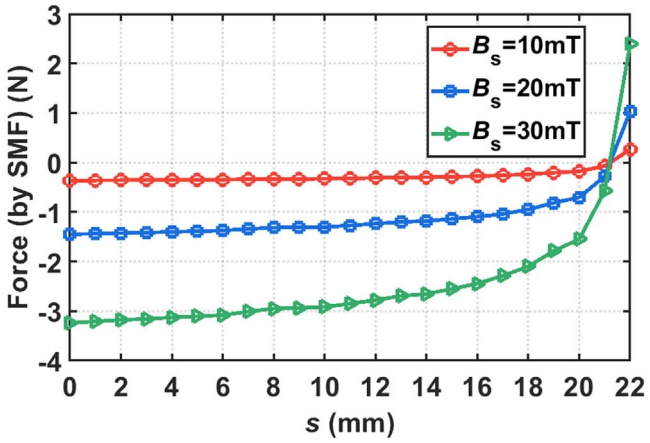

Figure 5. Electromagnetic force exerted on the armature by the SMF with different displacements.

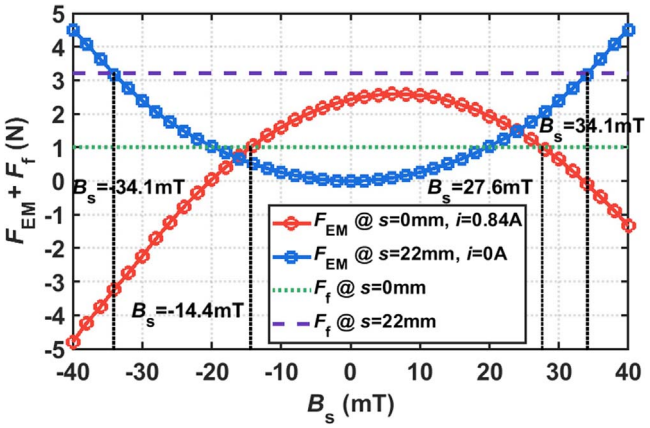

Figure 6. Total electromagnetic force (F_{EM}) and spring force (F_f) exerted on the armature under different SMFs.

More information can be found by calculating the total electromagnetic force under different SMFs as shown in figure 6, and the total electromagnetic force here refers to the force generated by the coil current and SMF together. In this paper, if the direction of the SMF is the same as the direction of the magnetic field generated by the LEA coil current, it is called a positive SMF, and the opposite is called a negative SMF. Two different cases are considered. The first is that the armature is at the initial position ($s = 0$ mm) and the coil current is at the rated value ($i = 0.84$ A), and the second is that the armature is at the contact point ($s = 22$ mm) and the coil current is removed. The reversed spring force (F_f) under these two cases are also provided in figure 6. For the first case, when the spring force is higher than the driving force, the armature will not move. Thus, the failure threshold during the closing process will be 14.4 mT for the negative SMF and 27.6 mT for the positive SMF. For the second case, when the spring force is smaller than the holding force, the armature cannot be pulled back to the initial position. Thus, the failure threshold during the opening process will be 34.1 mT for both directions.

SMF will also influence the equivalent inductance due to the saturation effect. Figure 7 shows the equivalent

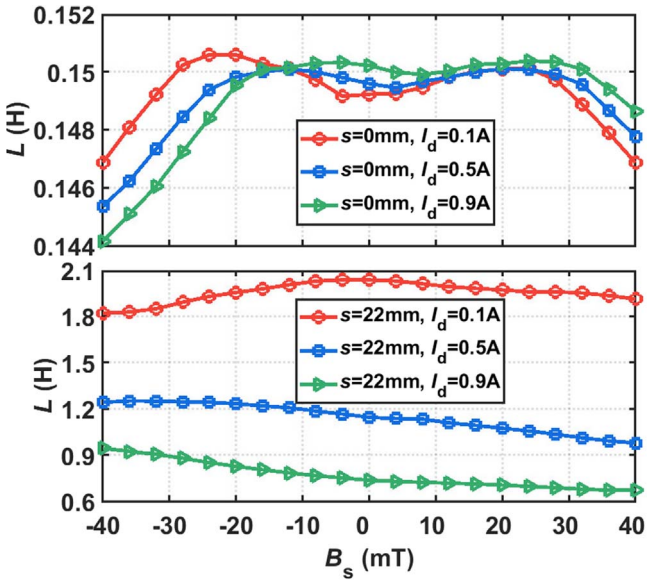

Figure 7. Equivalent inductance of the driving coil under different SMFs.

inductance (L) of the driving coil under different SMFs and driving currents. Two different cases, namely armature at the initial position ($s = 0$ mm) and at the contact point ($s = 22$ mm), are considered. As shown in figure 7, the equivalent inductance varies only a little under different SMFs and driving currents when the armature is at the initial position, with a maximum deviation about only 4%. This is because the gap is large and the saturation effect is not obvious. When the armature is at the contact point, the equivalent inductance increases a lot as the reluctance decreases, and it gets very sensitive to the SMF and driving current. The maximum deviation is 10.6% for $i_d = 0.1$ A, 14.6% for $i_d = 0.5$ A and 28.2% for $i_d = 0.9$ A.

2.3. Influence on starting current and release current

As the SMF will deviate the driving force or holding force applied on the armature as shown in figure 6, the starting current and release current will also be deviated by the SMF as they come from the force balance. Figure 8 shows the starting current (I_{st}) and release current (I_{re}) of the selected LEA under different SMFs. It is shown that the starting current increases with the strength of the SMF, and the starting current in the negative SMF is higher than that in the positive SMF. It indicates that the negative and positive SMFs have similar influence on the LEA, but the influence of the negative SMF is more significant, and the reason is explained in [9].

For the release current, it increases rapidly with the field strength in the negative direction when the field strength is over 20 mT. When the field strength increases from −20 mT to 40 mT, the release current decreases slowly and gets to zero at about 34 mT. It indicates that the armature will not be pulled back by the spring force when the field strength is over 34 mT, even though the coil current is totally removed. From figure 8, it is known that feeding a reversed coil current will

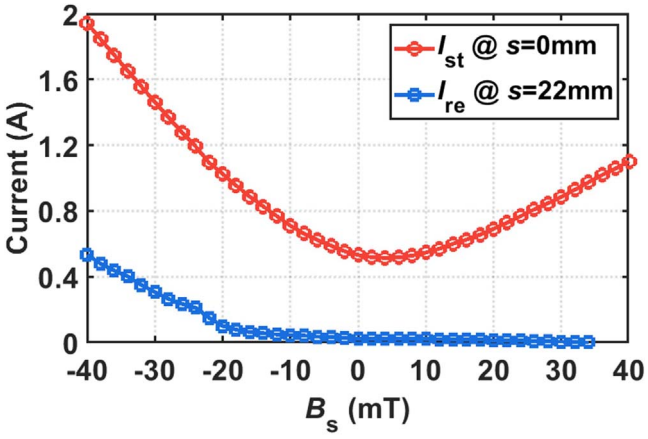

Figure 8. Starting current and release current under different SMFs.

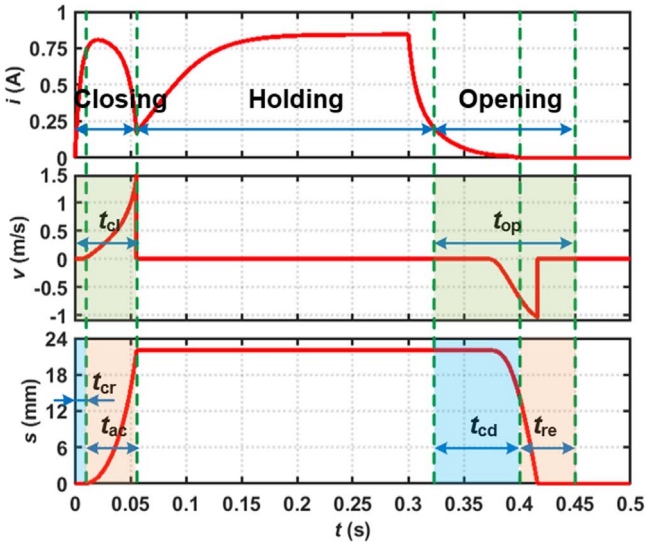

Figure 9. Characteristic curves of driving current (i), velocity (v) and displacement (s) during the whole operation duration under the rated operation parameters with no SMF.

help to release the armature in high SMFs as it will compensate the magnetic field generated by the SMF.

3. Dynamic performance of the LEA in the SMF

3.1. Performance of the LEA with no SMF

To get the dynamical characteristics of the LEA, a simulation model is built in Simulink to solve equations (1)–(6). Figure 9 shows the curves of driving current, velocity and displacement during the entire operation process under the rated parameters with no SMF. In the analysis, the source voltage (U_0) is set to 25 V, the resistance in the freewheel branch (R_f) is set to 50 Ω, and the driving voltage is applied at $t = 0$ ms and lasts for 300 ms. The closing process starts when the driving voltage is applied, and ends when the armature hits the top. As described in section 2, the closing process can be divided into two phases, namely current rising phase, during which the coil current rises to the starting current, and action

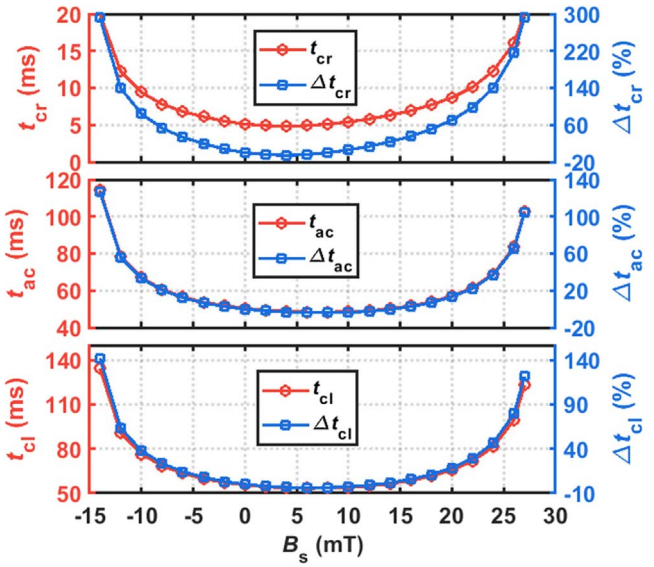

Figure 10. Current rising time, action time, total closing time and their deviations under the rated driving voltage and different SMFs.

phase, during which the armature moves until it reaches the contact point. The time spent in these two phases are called current rising time (t_{cr}) and action time (t_{ac}), respectively. For the LEA selected in the analysis, the current rising time is 5.1 ms and the action time is 50.4 ms, which contributes to a total closing time (t_{cl}) at 55.5 ms.

The opening process starts when the driving voltage is removed, and ends when the armature returns to the initial position. It can be also divided into two phases, namely current decay phase and returning phase. During the current decay phase, the coil current is governed by equation (5) and drops to the release current. During the returning phase, the armature will be pulled back to the initial position by the spring force. The time spent in these two phases are called current decay time (t_{cd}) and returning time (t_{re}), respectively. For the LEA selected in the analysis, the current decay time and returning time are 72.0 ms and 44.4 ms, respectively, which contribute to a total opening time (t_{op}) at 116.4 ms. It is obvious that increasing the freewheel resistance and decreasing the holding current by chopping will reduce the current-decay time.

3.2. Influence of SMF on closing process

With the simulation model built in Simulink, the dynamical performance of the LEA in different SMFs can be evaluated. Figure 10 shows the current rising time (t_{cr}), action time (t_{ac}) and total closing time (t_{cl}) under different SMFs when the rated driving voltage is applied. The deviations with respect to the value when no SMF exists are also provided. As the LEA will not move when the SMF is over the threshold, only the data in the range from –14 mT to 27 mT is given. It is obvious that t_{ac} is much larger than t_{cr}, and it contributes to 80%–90% of the total closing time. Besides, both t_{cr} and t_{ac} have a significant increase when the SMF has a certain strength. At the negative operation limit of −14 mT, t_{cl} will

increase to 134.3 ms, which indicates an increase of 142.0%. For the positive operation limit at 27 mT, t_{cl} will increase to 122.9 ms, with an increase of 121.6%.

At the beginning of the closing process, the coil current rises with a time-constant $\tau = L/R$, thus, t_{cr} is mainly determined by the starting current and the time constant. As shown in figure 7, the deviation of equivalent inductance under the impact of SMF is within 4%, which indicates that the equivalent inductance deviation has little influence on t_{cr}. On the other hand, the starting current is evidently deviated by the SMF as shown in figure 8. Thus, it is the main contributor of the deviation of t_{cr}. As the starting current resulted from the balance between the driving force and spring force, the force generated by the SMF is the primary cause for the deviation of t_{cr}. As shown in figure 5, in the majority of the armature displacement, the SMF will generate a reversed force on the armature, and it will slow the movement of the armature and contributes to the deviation of t_{ac}. This proves that the deviation of closing time mainly comes from the additional force generated by the SMF.

Figure 11 shows the current rising time, action time and total closing time under different driving voltages and SMFs, and the corresponding values under rated driving voltage and no SMF are also provided for reference. It is shown that increasing the driving voltage will help to reduce the closing time, and also to ensure the action of LEA in higher SMFs. It can be also observed that, if the LEA is exposed in a negative SMF with a strength of −40 mT, the total closing time is still longer than that of the rated condition even when it is driven by a voltage of 60.

As indicated in figure 8, the armature can be activated only when the coil current is over the starting current. Thus, the minimum required driving voltage (U_{min}) to ensure the successful activation of LEA in SMF can be evaluated by simply multiplying the starting current with the coil resistance. However, this minimum required voltage is not sufficient to ensure that the LEA acts within the rated time (55.5 ms, which is the closing time of the LEA without SMF). Thus, U_{norm} is defined in this paper, which refers to the voltage required to achieve a normal closing time under SMF. Figure 12 shows the U_{min} and U_{norm} under different SMFs. It can be observed that both U_{min} and U_{norm} in negative SMF will be higher than those in positive SMF because negative SMF exerts a greater force on the armature than the positive one. Besides, the difference between U_{min} and U_{norm} decreases when the SMF gets higher. When a SMF of −40 mT exists, the U_{min} and U_{norm} will be 57.5 V and 62.0 V, respectively, which are both over twice of the rated driving voltage.

Increasing the driving voltage will ensure the successful action of the LEA in high SMFs, however, it will also increase the driving power and the total energy dissipated in the driving coil. Taking a negative SMF of 40 mT, for example, a driving voltage of 62 V is required to ensure a nominal closing time, which indicates an increase of over 500% of the driving power. Besides, a higher driving voltage usually indicates a higher collision velocity or kinetic energy. As can be seen in figure 13, U_{norm} restores the LEA to the

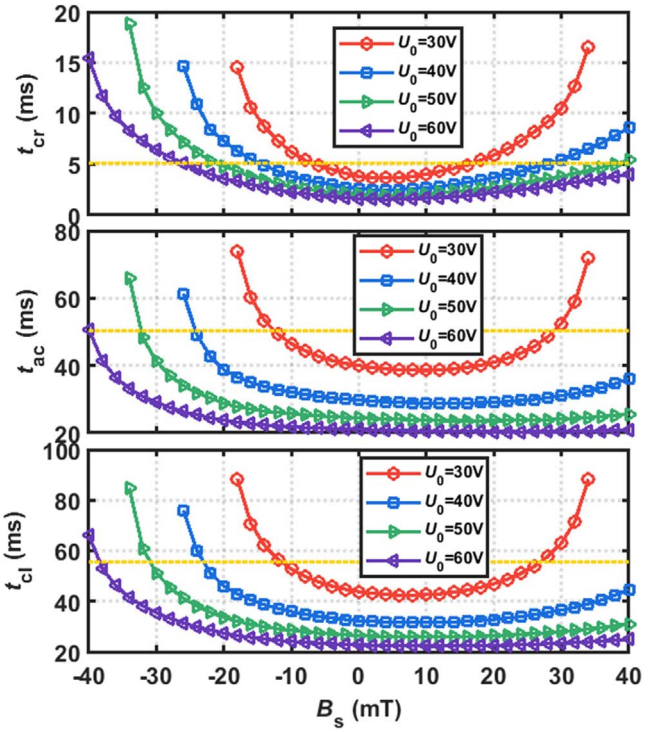

Figure 11. Current rising time, action time and total closing time under different driving voltages and different SMFs.

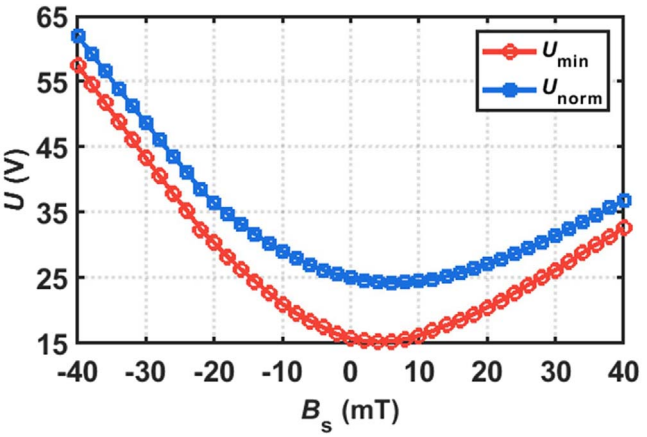

Figure 12. Minimum required driving voltage and suggested driving voltage of the LEA in different SMFs.

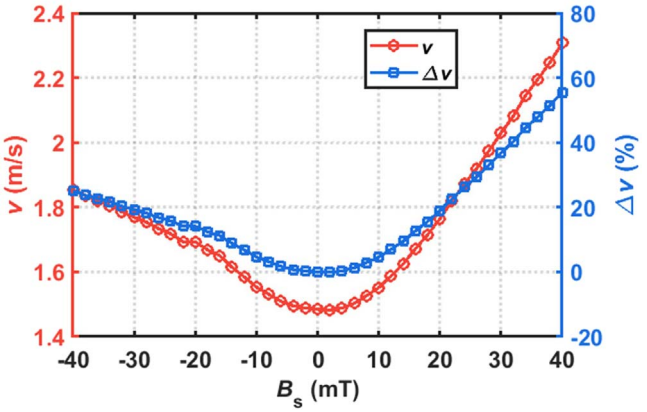

Figure 13. Collision velocity of the LEA under U_{norm}.

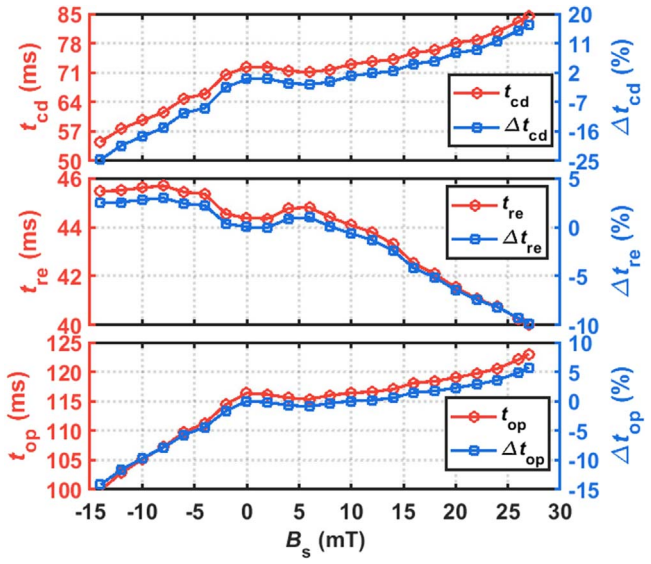

Figure 14. Current decay time, returning time, total opening time and their deviations under the rated driving voltage and different SMFs.

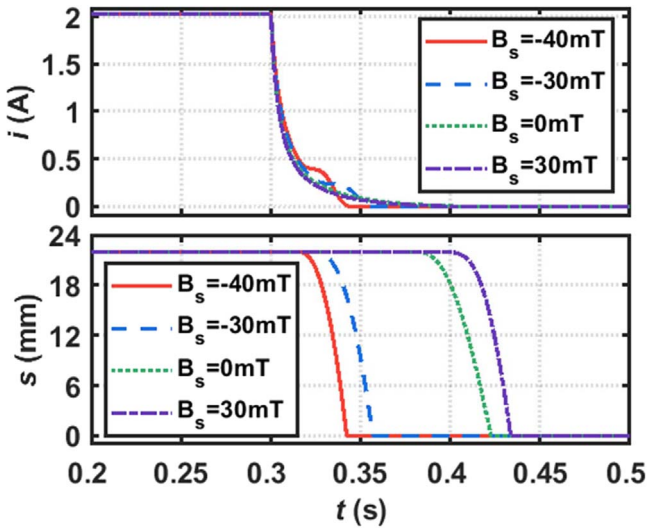

Figure 15. Coil current and displacement curves during opening process of some typical cases.

rated action time in the SMF, but also increases the collision velocity. Taking the case of 40 mT for example, the velocity is increased by 55%, with an increasement of 140% in kinetic energy. The increased collision velocity will lead to the contact bounce of the armature, which will threaten the reliability of the LEA, and complex control is needed under this situation [23, 27].

3.3. Influence of SMF on opening process

Figure 14 shows the current decay time (t_{cd}), returning time (t_{re}) and total opening time (t_{op}) under different SMFs when the rated driving voltage is applied. The deviations with respect to the value when no SMF exists are also provided. It is obvious that when the SMF increases from −14 mT to 17 mT, t_{cd} increases from 54.5 ms to 84.4 ms and t_{re} decreases from 45.7 ms to 40.0 ms. The maximum deviation of t_{cd} is −24.6% when the SMF is equal to −14 mT, and it is −9.8% for t_{re} when the SMF is equal to 27 mT. It indicates that the SMF has a stronger influence on t_{cd} than t_{re}. For the total opening time, it increases from 99.9 ms to 123.0 ms when the SMF varies from −14 mT to 27 mT, with a maximum deviation of 14.2% when the SMF is equal to −14 mT.

Figure 15 shows the coil current and displacement curves during the opening process of some typical cases, where the SMF is assumed −40 mT, −30 mT, 0 mT and 30 mT, respectively. As the LEA will fail in high SMFs, the driving voltage is assumed to be 60 V in the analysis to ensure the successful activation of the LEA. It is shown that, in higher negative SMFs, the current decay phase ends earlier as the release current is higher, which results in a smaller t_{cd} even though the equivalent inductance in higher negative SMFs is larger. This explains why t_{cd} is smaller in higher negative SMFs. As the release current comes from the balance between the holding force and spring force, the additional force generated by the SMF is the primary cause for the deviation of t_{cd}.

When the holding force gets lower than the spring force, the armature will be pulled back to the initial position. If ignoring the electromagnetic force applied on the armature, the motion of armature will be a simple harmonic vibration, and the time spent to return to the initial position will be

$$t_{re} = \arccos\left(\frac{d}{s_{max} + d}\right)\sqrt{m/k} = 36.0\ \text{ms}. \tag{14}$$

It is lower than rated returning time when no SMF exists as the residual holding force will slow the returning. As the force generated by the SMF is in the same direction as the spring force in most parts of the displacement, it will speed up the returning and reduce t_{re}. That is the case for the positive SMFs in figure 14. However, for the negative SMFs, the reduction is not obvious.

Figure 16 shows the current decay time, release time and total opening time under different driving voltages and different SMFs. It is shown that increasing the driving voltage will lead to a little increase of t_{cd} as it will increase the coil current. However, it has no influence of t_{re} as the returning phase starts at the release current, which is determined by the strength of the SMF, not the driving voltage. A strange phenomenon can be found: when the SMF is over 22 mT in the negative direction, t_{re} drops rapidly when the field strength increases. The inflection point coincides with the release current curve shown in figure 8. As shown in figure 15, when the armature is released in a high negative SMF, the coil current will be maintained at the release current. From equation (5), it is known that the induced voltage to maintain the coil current will be

$$\frac{\mathrm{d}[L \cdot i(t)]}{\mathrm{d}t} = L\frac{\mathrm{d}i(t)}{\mathrm{d}t} + i(t)\frac{\mathrm{d}L}{\mathrm{d}s}\frac{\mathrm{d}s}{\mathrm{d}t}. \tag{15}$$

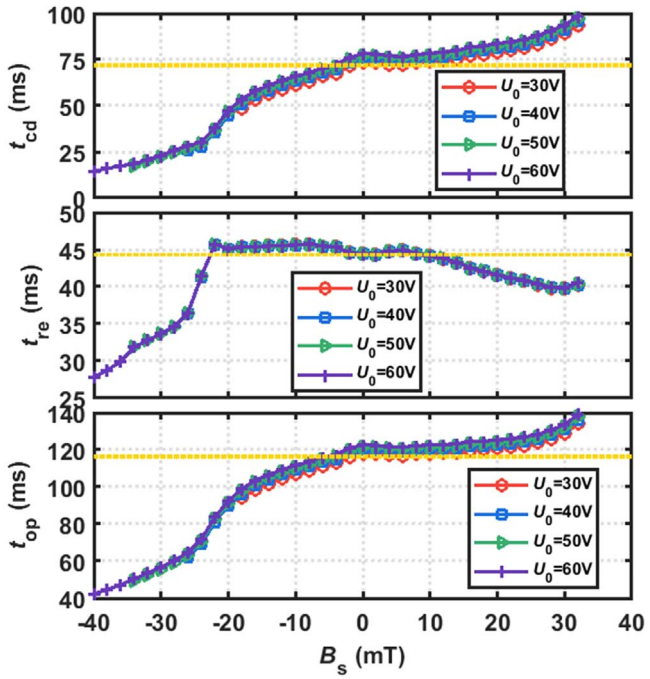

Figure 16. Current decay time, release time and total opening time under different driving voltages and different SMFs.

As the coil current remains unchanged during this period, the induced voltage will be proportional to the velocity of the armature. Thus, a higher release current will require a higher returning velocity, which will result in a shorter t_{re}. Further analysis shows that the unchanged release current and the high negative SMF will generate a high reversed force on the armature, and speed up the returning of the armature. In general, the positive SMF will slow down the opening process while the negative SMF will speed up the opening process, and the effect has a positive correlation with the field strength.

4. Validation experiment

To verify the proposed model and the analysis results, experimental tests were carried out on the magnetic field immunity test platform as shown in figure 17. The platform can generate a magnetic field of 200 mT, and the inhomogeneity η is 1.05, which meets the test method of ITER [28]. The real-time displacement of the armature of the LEA is measured by a CMOS type micro laser displacement sensor with a resolution of 10 μm as shown in figure 18.

Figure 19 shows the measured and simulated displacement curves of the LEA at −10 mT, 0 mT, and 10 mT respectively. The LEA is energized by a power supply operated at 25 V during 0 ms and 200 ms. The experimental and simulated results fit well except for some jitters due to the bounce of the armature when it collides with the iron core, which verifies the validation of the model proposed in this paper.

Figure 20 shows the simulated and measured closing time (t_{cl}) and opening time (t_{op}) of the LEA. It can be observed that the measured failure thresholds of the LEA are

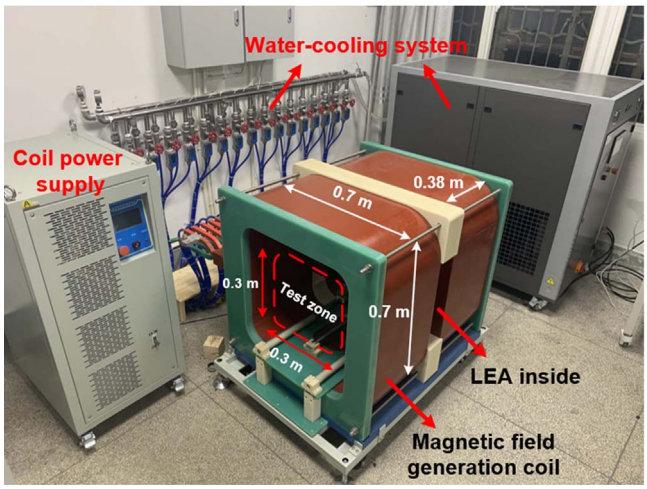

Figure 17. Magnetic field immunity test platform.

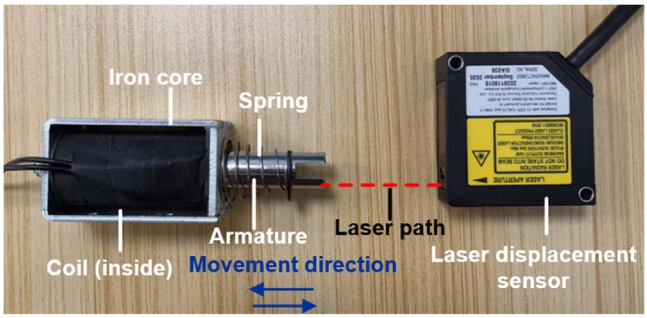

Figure 18. Laser displacement sensor and the LEA.

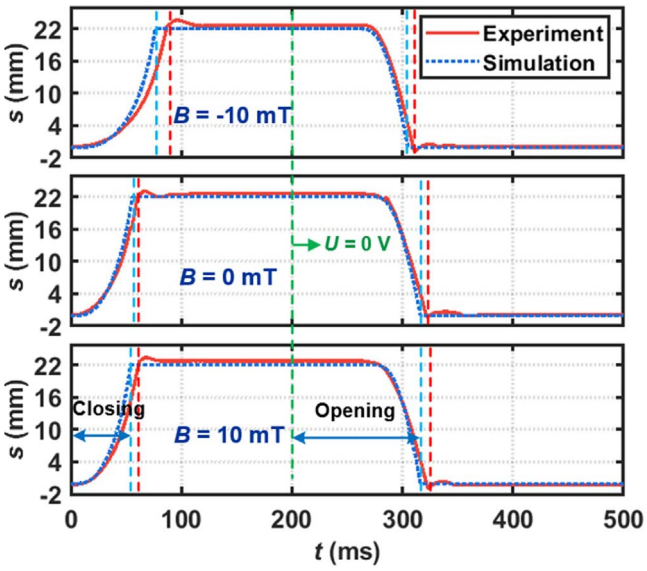

Figure 19. Comparison of experiment results and simulation results of the displacement wave.

−13 mT and 28 mT, which are slightly deviated from the simulation results (−14.4 mT and 27.6 mT). Therefore, compared with the experimental results, the simulation results have one more data of 14 mT and one less data of 28 mT in

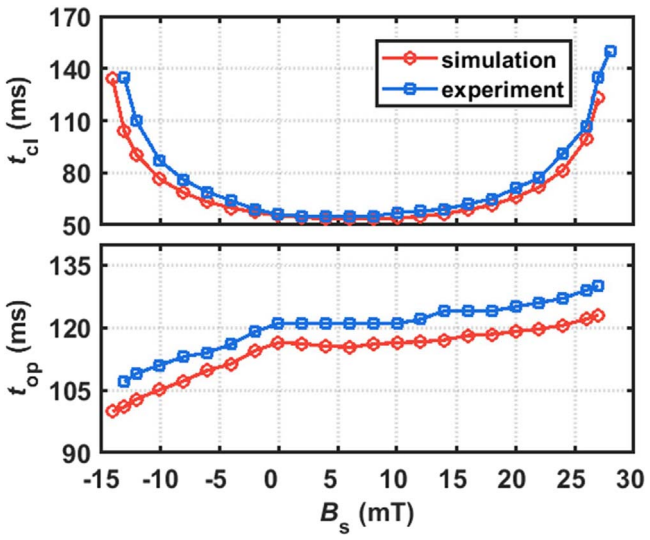

Figure 20. Simulated and measured closing time (t_{cl}) and opening time (t_{op}) of the LEA under different SMFs.

figure 20. For the closing process, deviation of the measured and simulated results increases with the increase of SMF. For the opening process, the deviation is stable at around 6 ms. The deviation is due to the friction force which is not considered in the model. For the closing process, the resultant force decreases with the increase of SMF strength, and the proportion of the ignored friction force in the resultant force increases, which results in a higher deviation at higher SMFs. For the opening process, since the coil is not energized, the spring force dominates, thus the deviation is stable. In general, the experimental results are in good agreement with the simulated ones, which also verifies the validity of the proposed analysis model and the analysis results in this paper.

5. Conclusions

In this paper, a multi-physics coupling model of LEA is proposed, the failure mechanism LEA in an SMF is revealed, and the influence of the SMF on the dynamic performance of the LEA is studied and quantified. Moreover, the effect of driving voltage on the LEA in the SMF is investigated. The main conclusions are summarized as follows:

(1) A multi-physics coupling model including magnetic field, electric circuit and mechanical motion is proposed, and its validation is verified by experiments.
(2) The influence of SMF on the driving force is proved to be the main reason that affects the dynamic characteristics of the LEA.
(3) SMF impedes the closing process of LEA, and the time-consuming is positively correlated with the SMF strength, and the effect of negative magnetic field is greater than that of positive magnetic field. However, for the opening process, a negative SMF facilitates the return movement while a higher positive SMF impedes it.
(4) Increasing the voltage will reduce the time of the closing process, but introduced the problem of increased power and energy, and also increased the probability of contact bounce. The opening process in positive SMFs can be facilitated by applying a reverse current.

Acknowledgments

This work is supported in part by the National Key R&D Program of China (No. 2017YFE0301800), in part by National Natural Science Foundation of China (No. 51821005), and in part by the Comprehensive Research Facility for Fusion Technology Program of China (No. 2018-000052-73-01-001228).

ORCID iDs

Rumeng WANG (王如梦) https://orcid.org/0000-0001-6282-2075

References

[1] Kozioziemski B J *et al* 2007 *Nucl. Fusion* **47** 1
[2] Benfatto I *et al* 2005 *Fusion Eng. Des.* **75–79** 235
[3] Roccella R 2019 *Static and Transient Magnetic Field Maps at level B1 Tokamak Complex* (Cadarache: ITER)
[4] Roccella M 2017 *Assessment of Magnetic Field and its Maximum Time Derivative in Tokamak Building* (Cadarache: ITER)
[5] Wang R M *et al* 2022 *J. Magn. Magn. Mater.* **550** 169125
[6] Hourtoule J *et al* 2005 *Fusion Eng. Des.* **75–79** 179
[7] De Lorenzi A *et al* 2005 *Fusion Eng. Des.* **75–79** 33
[8] Tripathy S *et al* 2020 *Energy* **193** 116740
[9] Wang R M *et al* 2021 *Fusion Eng. Des.* **167** 112344
[10] Tapia C C *et al* 2020 *Measurement* **166** 108174
[11] Lee J *et al* 2012 *Finite Elem. Anal. Des.* **58** 44
[12] Clark R E *et al* 2005 *IEEE Trans. Magn.* **41** 1163
[13] Li Y L *et al* 2020 *IEEE Trans. Magn.* **56** 7506004
[14] Zhai G F, Wang Q Y and Ren W B 2008 *J. Zhejiang Univ. Sci. A* **9** 577
[15] Yang W Y, Zhou X and Zhai G F 2007 *Trans China Electrotech Soc* **22** 179 (in Chinese)
[16] Wang R M *et al* 2022 *IEEE Trans. Plasma Sci.* **50** 4267
[17] Yang Y *et al* 2018 *IEEE Trans. Ind. Electron.* **65** 8204
[18] Fang S H, Lin H Y and Ho S L 2009 *IEEE Trans. Magn.* **45** 2990
[19] Smugala D 2021 *IEEE Trans. Ind. Electron.* **68** 6152
[20] Forrai A, Ueda T and Yumura T 2007 *IEEE Trans. Ind. Electron.* **54** 1430
[21] Lin H Y *et al* 2013 *IEEE Trans. Ind. Electron.* **60** 5148
[22] Chin C S and Wheeler C 2013 *IEEE Trans. Ind. Electron.* **60** 5315
[23] dos Santos Dias de Moraes P M and Perin A J 2008 *IEEE Trans. Ind. Electron.* **55** 861
[24] Espinosa A G *et al* 2008 *IEEE Trans. Ind. Electron.* **55** 3742
[25] Tang L F, Han Z P and Xu Z H 2021 *IEEE Trans. Ind. Electron.* **68** 6064
[26] Hey J *et al* 2014 *IEEE Trans. Ind. Electron.* **61** 5453
[27] Ramirez-Laboreo E, Sagues C and Llorente S 2017 *IEEE Trans. Ind. Electron.* **64** 535
[28] Rao Y 2016 *Test Method for ITER Equipment for Static D.C. Magnetic Fields* (Cadarache: ITER)